Multi-Spectral Automated Rotating Shadowband Radiometry

L. Harrison
Atmospheric Sciences Research Center
State University of New York at Albany
Albany, NY 12205

I am developing two related instruments for use in the Atmospheric Radiation Measurement (ARM) program; both use an automated rotating shadowband technique to make spectrally resolved measurements of the direct-normal, total horizontal, and diffuse horizontal irradiances. These parameters of the sky-radiance function are measured using the same detector (for a given wavelength), eliminating the difficulties inherent in comparing these data when measured by independent detectors.

The first of these instruments uses independent interference-filter/photodiode detectors to measure any seven wavelength bands chosen between 350 nm and 2.5 μm. Nine of these multiple filter instruments are currently deployed as part of the U.S. Department of Energy's (DOE) Quantitative Links measurement program. This instrument has been selected for deployment in the spring of 1992 at the extended field sites of the first Cloud and Radiation Testbed (CART) installation.

The second instrument uses a prism spectrograph and a Charge-Coupled Device (CCD) photodiode array to measure 256 wavelength intervals from 370 nm to 1 μm. This instrument, which is at the prototype stage, is intended for deployment at the central sites.

In this abstract, I describe the technical features of these two instruments and discuss data recovery and interpretation for sky conditions in which single-scattering dominates.

The Multi-Filter Rotating Shadowband Radiometer

The basic geometry of the rotating shadowband radiometer (RSR) can be seen in Figure 1. The detector consists of a diffuser-integrator that illuminates a hexagonally close-packed array of seven photodiode-interference-filter assemblies. The function of this diffuser is to produce a cosine detector response with respect to the angle of any incident beam measured from the zenith; this is equivalent to measuring the flux incident on a horizontal plate. These diodes are mounted to internal electronics that implement a separate transconductance amplifier (zero-bias current-to-voltage amplifier) for each of the photodiodes.

The photodiodes are operated in the photovoltaic (rather than photoconductive) mode to reduce noise. The amplifiers are implemented using individual commutating-auto-zero (i.e., "chopper stabilized") devices to reduce variations in input offset and bias current. The board also implements a precision (0.1°C) temperature controller that stabilizes the temperature of the entire detector assembly.

Temperature stabilization is necessary to improve the accuracy at several stages. Both the bandpass and transmission of interference filters are sensitive to temperature, although these effects are most pronounced with bandpasses that are significantly narrower than those we employ. More important, the photodiodes exhibit changes in sensitivity with temperature, and the bias currents of the amplifiers are temperature-sensitive as well. Further, a simple effect that is often neglected is that the "gain" of the current-to-voltage amplifier is controlled by the absolute resistance of the feedback, rather than by the ratio of two resistances, as is the case with the more commonly used voltage gain circuits. Temperature control of the entire assembly eliminates all of these undesirable effects.

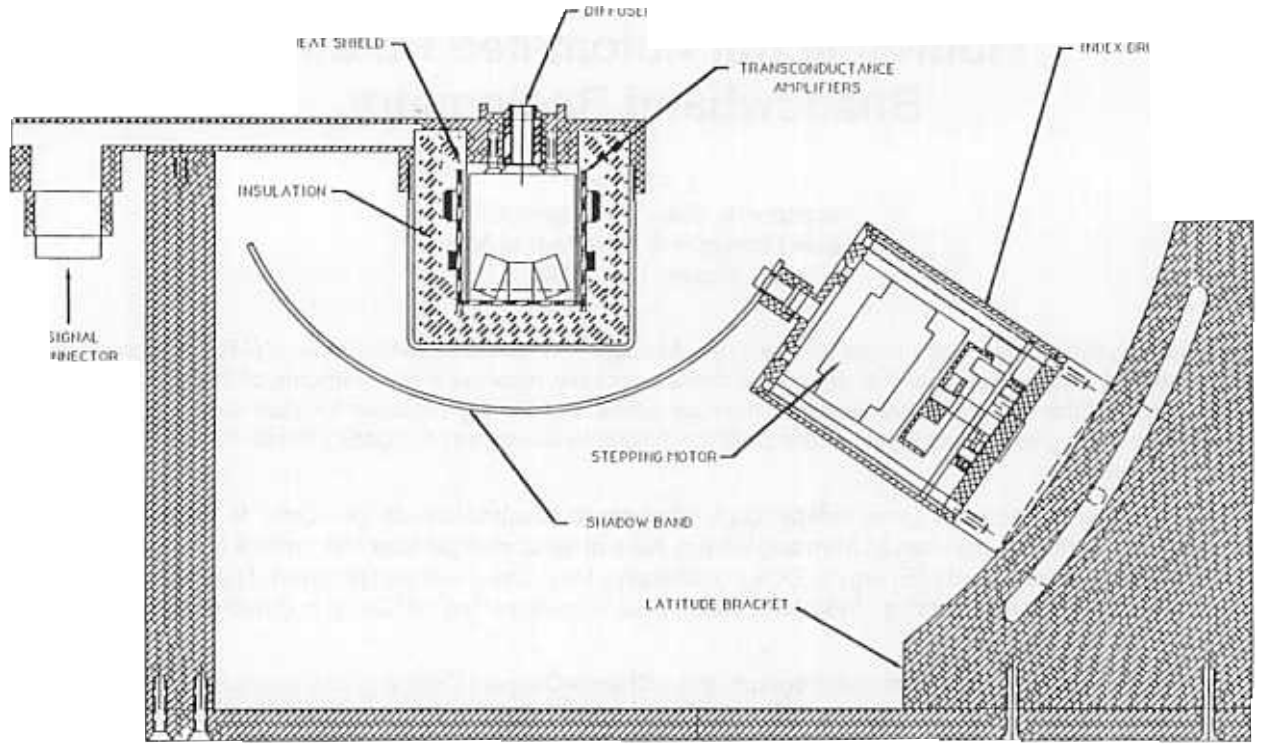

Figure 1. Multi-Filter Rotating Shadowband

The photodiodes are operated in the photovoltaic (rather than photoconductive) mode to reduce noise. The amplifiers are implemented using individual commutating-auto-zero (i.e., "chopper stabilized") devices to reduce variations in input offset and bias current. The board also implements a precision (0.1°C) temperature controller that stabilizes the temperature of the entire detector assembly.

Silicon photodiodes are optimum over the wavelength range of 300 to 1000 nm. We currently use DF-XXX series integrated photodiode-interference-filter assemblies manufactured by EG&G. Beyond 1050 nm, either Germanium or Indium-Gallium-Arsenide (InGaAs) photodiodes are required. Bandpasses greater than 20 nm are needed at wavelengths beyond 1.6 μm.

The shadowing band is a strip of metal formed into a circular arc that lies along a celestial meridian (the face of the detector is the center for this arc). It can be precisely rotated (0.4°) around the polar axis by a stepping-motor that is in turn controlled by a microprocessor. This band blocks a strip of sky with a penumbral angle of 8°, more than sufficient to block the solar disk. The instrument permits a simple mechanical adjustment to align the polar axis with the earth's axis; this alignment is done when the instrument is installed at a site. No further mechanical adjustment is necessary.

The operation of the instrument is controlled by its self-contained microprocessor. At each measurement interval, the microprocessor computes the solar position using an approximation for the solar ephemeris developed by Michalsky (1988). The measurement sequence starts with a measurement made while the band is at the nadir; this is the total horizontal irradiance. The band is then rotated to make three measurements in sequence: the middle one blocks the sun and the other two block strips of the sky 6° to either side. These side measurements permit a correction for the "excess sky" blocked by the band when the measurement that blocks the sun is made; the average of these two side measurements is subtracted from the total

horizontal measurement; this correction is then added to the sun-blocked measurement to determine the diffuse irradiance. Finally, the diffuse component of the irradiance can be subtracted from the total horizontal to produce the direct beam component; this in turn can be corrected by the known cosine of the solar position from the zenith angle (available from the ephemeris calculation) to produce the direct beam flux on a normal surface. The entire measurement sequence is completed in less than 10 seconds and is normally programmed to occur four times per minute.

The microprocessor also acts as a "data logger," accumulating the data from the shadowband measurements, as well as ancillary measurements from other instruments, if desired. The instrument can average over selected intervals; note that in this case the summation of the direct normal component is done subsequent to the application of the cosine-angle correction (done individually for each measurement). This is necessary to produce correct results at high zenith angles where the cosine varies rapidly.

The basic design of this instrument has several advantages compared with the alternative of using two detectors: one fixed to measure the total horizontal irradiance, and one mounted on a tracking mechanism to measure the direct normal component (thus requiring a narrow field of view). The RSR is simpler, less expensive, and more robust. Further, the three components are derived from a single optical detector, greatly reducing intercalibration worries about both absolute sensitivity and spectral bandpass, and guaranteeing that the measurements are synchronous. These features improve the utility of calibration via Langley extrapolation, since the measurements of the diffuse and total horizontal components are calibrated as well. Data from a multi-filter instrument are shown and discussed below.

The CCD Array Spectrometer

I am also working on a higher resolution detector consisting of a prism spectrograph coupled to a CCD array (see Figure 2). This instrument has not yet been deployed for field testing; consequently, it will be described only briefly here.

The prism spectrograph for this instrument is geometrically conventional, but is unusual in using quartz for all optical surfaces. The nominal wavelength range is 350 to 1050 nm, although this can be adjusted by changing the

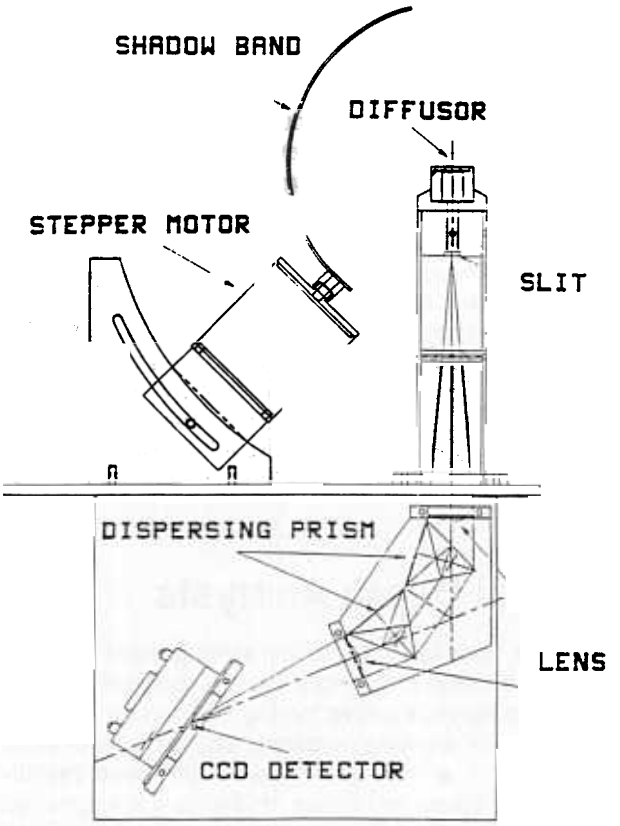

Figure 2. CCD Array Rotating Shadowband

focal length of the final lens and repositioning the detector array. The detector is a 256-element linear CCD Silicon Photodiode array manufactured by Hammamatsu. The corresponding spectral resolution per pixel is 0.6 nm at 350 nm, and nearly 12 nm at 1050 nm.

The spectrograph uses all-quartz optics to permit observations below 400 nm. Neither flint achromats nor flint dispersing prisms can be employed, and careful optical tradeoff studies were necessary to arrive at an acceptable design. The solution is straightforward to construct; it uses only simple plano-convex lenses, and coma and spherical aberrations are controlled by making the f-number of the system ≈ 7. Chromatic aberration "controls itself" because the prism material is identical to that of the lenses, and the lenses are not chromatically corrected. The result is that the entire effect of chromatic aberration manifests itself as a planar tilt in the focal surface of the dispersed spectrum,

which can be readily accommodated simply by tilting the detector.

Alternatives based on air-spaced quartz achromats become coma-limited at *f* numbers less than approximately 4.7, a negligible improvement, given significantly increased complexity. Grating instruments have difficulties not discussed here. In any case, a typical *f* number for small single-grating spectrographs is 3.5; thus, the prism design shown here is only a factor of 4 slower in light throughput than any likely grating instrument. We built a prototype of this instrument, which has been tested both by examining the output spectra by eye and by displaying the results measured with the CCD array. We believe these results constitute "proof of principle" that this instrument will perform as described; however, significant development effort remains to make this instrument ready for routine operation.

Optical Depth Analysis

The data from the RSR instruments provide spectrally resolved surface irradiances that are needed to understand shortwave radiative forcing and can be used for a wide range of analysis purposes. The analysis of cloudy conditions in an attempt to derive improved radiative parameterizations for climate models and the accumulation of "subgrid" statistical (both spatial and temporal) properties of the radiative transfer in a wide range of regimes are of particular importance to ARM. These analyses are complicated and will depend on other measurements, including measurements taken by the RSR instruments; they are too complex to discuss here.

Instead, I wish to discuss the more straightforward analysis of data taken when single-scattering dominates the radiative transfer—these conditions are of interest to the Instantaneous Radiation Transfer Experiment (IRTE). They permit the direct inference of the optical depth as a function of wavelength, $\tau(\lambda)$ (from which column-integral aerosol properties can be inferred) and a long-term "built-in" calibration of the instrument against the solar constant.

The plot in Figure 3 shows a day of observations taken by a multi-filter RSR operating at Rattlesnake Mountain Observatory (RMO) at latitude 46.40° N, longitude 119.60° W, elevation 1100 m. The instrument has the "Quantitative Links" complement of detectors (see the table in the next section); these data are for wavelength channel 3 where λ = 500 nm, with 10 nm full-width-at-half-maximum bandpass. Note that the irradiance scale shown is uncalibrated (it is simply mV of output), but the shadowband technique guarantees that all three components are identically scaled. Consequently, we can analyze the direct-normal data to obtain a calibration of the detector against the sun's output and then apply this calibration to the diffuse and total horizontal components.

The ≈ 10 nm bandpasses are chosen so that curve-of-growth problems are avoided. The extinction of the direct-beam component of the irradiance obeys Lambert's law, $I/I_o = e^{-\tau A}$, at all wavelengths other than the water vapor channel at 940 nm.[a] (t is the optical depth per unit airmass and A is the number of airmasses along the optical path.) The airmass changes during the day because the pathlength through the atmosphere changes as the sun rises and sets.

Consequently, we can attempt a linear regression of the logarithm of received intensity versus airmass (that can be calculated from the time of observation and the location) to yield τ directly. This method is known as Langley analysis. A critical assumption is required: the optical properties of the atmosphere that govern t must remain stable during the time needed to accumulate the range of airmasses used for the regression. However, if this assumption is violated, it usually produces evident curvature of the plotted data points.

The plot for this regression applied to the data above is shown in Figure 4. Note that we get an excellent straight line fit, provided that we can ignore the evident "dips" associated with small cloud passages evident in the time series above.

τ is simply the negative of the slope of the regression line. Perhaps equally useful is the extrapolated intercept of this regression with zero airmass, Izero. This value is the inferred solar constant at this wavelength. Obtaining this value requires an extrapolation of at least one airmass, and so small errors in t can alter the value of Izero by several percent. Individual regressions do not constitute a suitable calibration unless made under remarkably good conditions (e.g., at Mauna Loa). However, these variations are not systematic, and by averaging the results of a series

(a) The water vapor channel is fully saturated and exhibits square root curve-of-growth. This permits a standard regression to yield the column water vapor (Guzzi 1985), an important atmospheric variable for radiative transfer models and the purpose of providing this measurement wavelength.

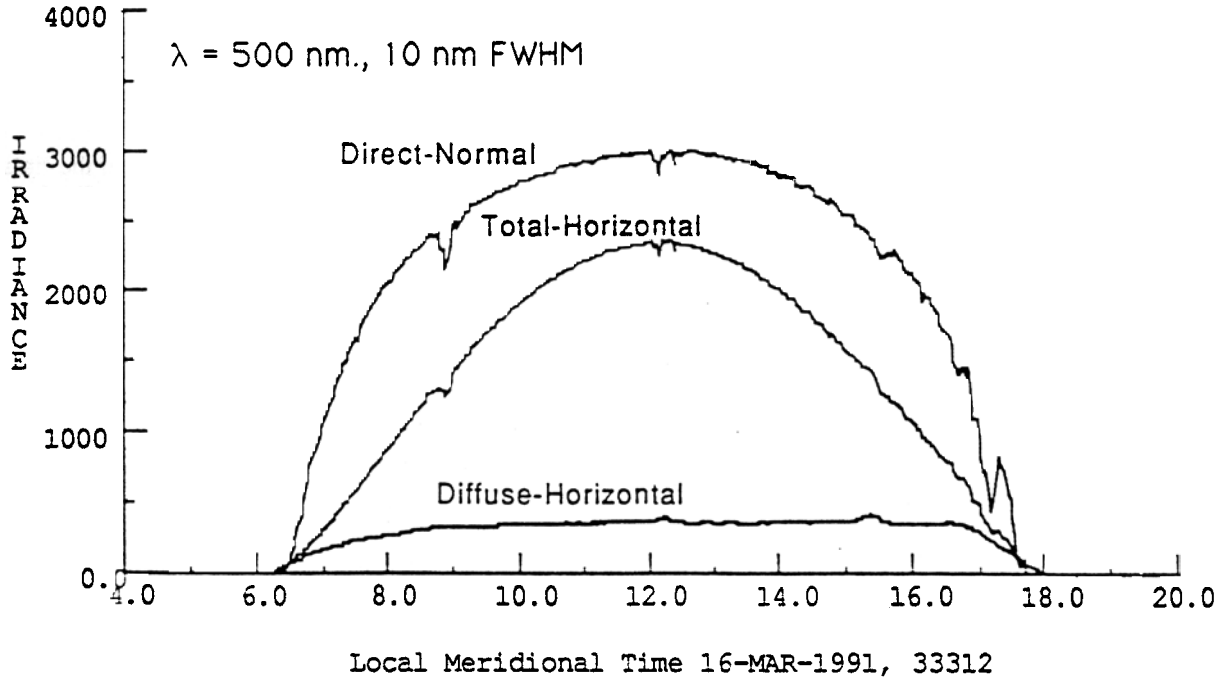

Figure 3. Observations Taken by a Multi-Filter Rotating Shadowband Radiometer Operating at Rattlesnake Mountain Observatory on 16 March 1991.

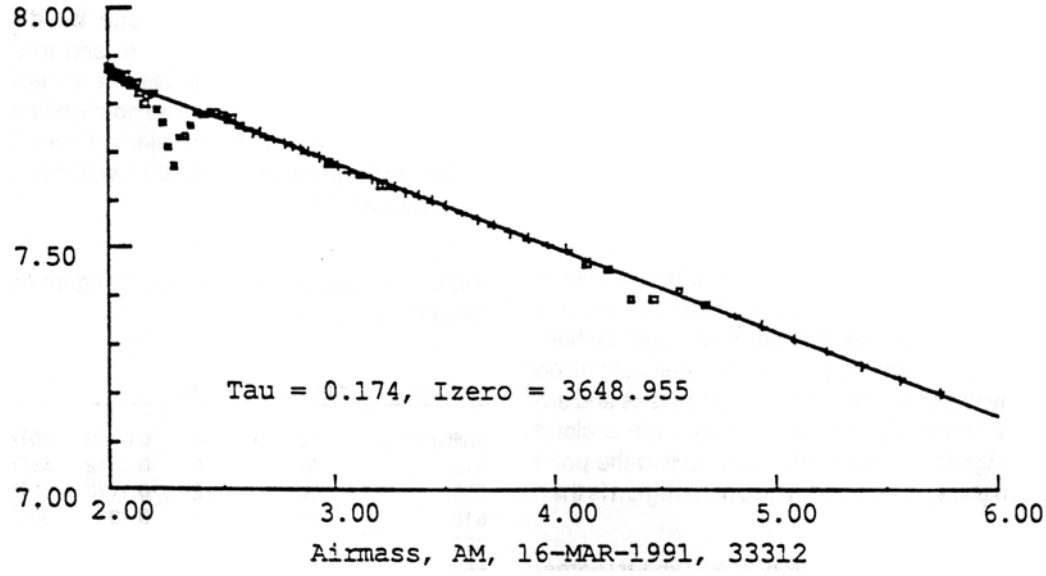

Figure 4. Plot of Linear Regression of the Logarithm of Received Intensity Values Versus Airmass or Data Collected at Rattlesnake Mountain Observatory on 16 March 1991.

of daily regressions (adjusting for the slow annual variation in the earth-sun distance), we can make accurate calibrations against the solar constant.

An Objective Langley Regression Algorithm

The simple-minded notion of using a least-squares regression on all the data only works under perfect sky conditions—e.g., Mauna Loa. Elsewhere, cloud transients (even thin cirrus) will produce "dips" such as those shown above. These must be removed or the regression will produce nonsense results.

To date, this has been done by subjective editing; a scientist examines the data graphically and determines which points should be used for the regression. Aside from being quite labor-intensive, this process is subject to criticism that differing analysts may arrive at different results and that analysts often cannot give useful descriptions of what "algorithm" they use to decide which points should be kept and which rejected.

In contrast, the data above were processed using an automated objective algorithm. This algorithm operates as follows: it first scans the data series to find intervals (either morning or afternoon) where the airmass ranges from 2 to 6. Lower airmasses are not used (even if available in the data) because the rate-of-change of the airmass is small, creating a greater opportunity for changing atmospheric conditions to affect the regression. Higher airmasses are avoided because of the uncertainty caused by refraction corrections that are increasingly sensitive to atmospheric temperature profiles.

The algorithm then operates on the data with a series of filters to remove erring measurements. The first filter is a delta-difference derivative filter that identifies regions where the slope of dI/d(Airmass) is positive. These cannot be produced by any uniform airmass turbidity process and are evidence of the "recovery" of the intensity from a cloud passage. The algorithm then "folds back" to find the point where the cloud passage started. The entire region is then eliminated.

Two iterations are then made of a robustified linear regression. After each iteration the points that lie more than 1.5 standard deviations from the regression are removed. Points that are used to compute the final Langley regression are marked by a simple "plus." Points discarded as cloud passages or outliers are marked as a box.

The results for the morning regression of the data for all seven wavelength channels are shown in Table 1.

Both the unfiltered silicon photodiode, and the bandpass at 940 nm are affected by curve-of-growth behavior due to H_2O; hence, these estimations are not strictly correct. The water band at 940 nm causes the optical depth to be much larger than it would be if there were no gas absorption. Note also that the value for s, the standard deviation of the residuals, is computed using the variance of the ln(I).

To validate this algorithm, I have compared its values for the optical depth with previous subjective analysis my colleague Dr. J. Michalsky performed on data taken at the National Oceanic and Atmospheric Administration (NOAA) laboratory in Boulder, Colorado, using a single-channel photopic bandpass RSR. I will discuss this intercomparison of analysis methods in more detail in a paper I am preparing, but the basic conclusions are

- The objective algorithm successfully retrieves an optical depth that compares with the subjective analysis to an RMS variation of < 0.01 in 93% of the cases.
- The "outlier" comparisons can be discriminated by setting threshold values for s, and the fraction of the data points discarded. If cases are discarded where $\sigma > 0.005$ or more than half the points within the measurement window have been rejected, then the RMS variation in τ is on the order of 0.001, with a worst-case "error" of about 0.025.

Table 1. Regression of the Data Using an Automated Objective Algorithm

λ(nm)	# points	# kept	τ	I_0	
unfiltered Si	66	34	0.0758	3074.9092	0.0033
415	66	40	0.3162	4854.4395	0.0035
500	66	32	0.1778	3673.3503	0.0018
610	66	32	0.1311	3517.5959	0.0015
665	66	34	0.0799	2769.0618	0.0013
862	66	24	0.0177	2982.5334	0.0015
940	66	35	0.1120	4134.3071	0.0086

These data, taken at Boulder, are a difficult test for this analysis algorithm, in part because Boulder is known to be a difficult site due to rapidly varying cloud patterns and because these data 5-minute averages of 15-second samples. We normally recommend that data used for Langley analysis be single observations; the delta-difference filter is much more effective in such cases. Consequently, we expect similar comparisons done elsewhere to yield equivalent or better results.

Conclusions

The multi-filter RSR instruments are ready for field use and will provide spectrally resolved direct-normal, diffuse horizontal, and total horizontal irradiance measurements for the ARM program. An important advantage of this method is that the diffuse and total irradiance measurements are guaranteed to have the same bandpass and sensitivity as the direct-normal irradiances, and, thus, to share the utility of Langley calibration.

An objective analysis algorithm has been developed to perform the Langely regressions. This algorithm has been validated by comparison with subjective reduction and demonstrates an accuracy of 0.01 optical depth with a retrieval efficiency of 93%. (This is a retrieval efficiency of "possible" days as defined by the subjective analysis, not a fraction of all events.) ARM will need an automated algorithm; the quantity of data to be analyzed simply cannot be managed by subjective methods that depend on human examination of each datum.

References

Guzzi, R., G. C. Maracci, R. Rizzi, and A. Sicardi. 1985. "Spectroradiometer for Ground-Based Measurements Related to Remote Sensing in the Visible from a Satellite." *Applied Optics* 24:2859-2863.

LeBaron, B. A., J. J. Michalsky, and L. Harrison. 1989. "Rotating Shadowband Measurement of Atmospheric Turbidity: A Tool for Estimating Visibility." *Atmos. Environ.* 23:255-263.

Michalsky, J. J. 1988. "The Astronomical Almanac's Algorithm for Approximate Solar Position." *Solar Energy* 40:227-235.

Michalsky, J. J., L. C. Harrison, and B. A. LeBaron. 1987. "Empirical Radiometric Correction of a Silicon Photodiode Rotating Shadowband Radiometer." *Solar Energy* 39:87-96.